

Eddy contributions to the meridional transport of salt in the North Atlantic

A. M. Treguier,¹ J. Deshayes,¹ C. Lique,² R. Dussin,³ and J. M. Molines³

Received 27 January 2012; revised 21 March 2012; accepted 21 March 2012; published 5 May 2012.

[1] The meridional transport of salt in the Atlantic ocean is an important process for climate, controlling the stability of the meridional overturning circulation. The contribution of transient eddies to this transport is quantified in an eddy resolving North Atlantic model at $1/12^\circ$ resolution (NATL12), and compared with lower resolution North-Atlantic and global $1/4^\circ$ models. In NATL12 between 10°N and 40°N , there is a volume loss by evaporation of 0.6 Sverdrups (Sv). The divergence of the eddy flux of salt (normalized by a reference salinity of 34.8) is 0.2 Sv over the region, a significant fraction of the total air-seawater exchange, but it is compensated by an opposite convergent transport of salt by the mean flow, so that the total transport of salt is small. The compensation between eddy and mean salt transport is almost complete in a multicentury long global model experiment, but less effective in NATL12 because the short integration time does not allow the salt content to equilibrate and the model drift is large. Eddies arising from baroclinic instability contribute to the meridional salt transports at the northern and southern boundary of the subtropical gyre, where they appear consistent with a lateral diffusion acting on the mean salinity gradient. However, the eddy transport of salt is the sum of two terms: an advective contribution (arising from the correlations of velocity and isopycnal thicknesses) and a diffusion along isopycnals. Both components have the same amplitude at the southern boundary of the subtropical gyre, while diffusion is dominant at the northern boundary.

Citation: Treguier, A. M., J. Deshayes, C. Lique, R. Dussin, and J. M. Molines (2012), Eddy contributions to the meridional transport of salt in the North Atlantic, *J. Geophys. Res.*, 117, C05010, doi:10.1029/2012JC007927.

1. Introduction

[2] The meridional transports of heat and salt by the ocean are key mechanisms that influence the global climate. The ocean contributes to the heat transport from the tropics to high latitudes, and this heat transport can be a source of climate variability on seasonal, decadal and longer time-scales. The role of the meridional transport of salt has been highlighted recently in coupled climate models, because the freshwater input at the southern boundary of the Atlantic ocean appears to be an indicator of the bistability of the meridional overturning circulation [Huisman *et al.*, 2010; Hawkins *et al.*, 2011]. The net meridional transport of salt would vanish in a steady state ocean because evaporation and precipitations do not carry any salt. In a changing climate, regional variations of the salt content are expected to

occur, and these can be related to changes in the meridional transports or/and changes in the regional balance of evaporation, precipitations and continental runoff. In the North Atlantic ocean such changes may have huge consequences because of the feedbacks involved in the global thermohaline circulation, driven by the formation of North Atlantic Deep Water. Curry *et al.* [2003] show that the salinity of the subtropical Atlantic has increased from the fifties to the nineties, while the subpolar Atlantic freshened. The origin of these changes cannot be fully understood without better estimates of oceanic transports of salt.

[3] Transports of heat or salt are products of a velocity and a scalar, and as a result the time averaged transport has a contribution from the averaged correlations between velocity and temperature (or salinity) anomalies. These terms are usually called “eddy transports”. In the atmosphere, transient disturbances arising from baroclinic instability of the zonal mean flow are a major contribution to the meridional transport of energy at mid latitudes, as explained for example by Kuo [1956]. A recent estimate of the atmospheric eddy heat flux is found in Trenberth and Stepaniak [2003], who discuss the tendency for the meridional heat transport by stationary waves and by transient eddies to cancel each other, a phenomenon first pointed out by van Loon [1979]. In the ocean, observations are sparse and the contribution of transient eddies to the meridional transport of heat has been

¹Laboratoire de Physique des Océans, CNRS-Ifremer-IRD-UBO, Plouzane, France.

²Joint Institute for the Study of Atmosphere and Ocean, University of Washington, Seattle, Washington, USA.

³LEGI, Grenoble, France.

Corresponding Author: A. M. Treguier, Laboratoire de Physique des Océans, CNRS-Ifremer-IRD-UBO, BP 70, Plouzané F-29280, France. (anne.marie.treguier@ifremer.fr)

evaluated using numerical models. A pioneering study is that of *Cox* [1985], who was the first to show that the transport by eddies and by the mean flow change in opposite directions when the model resolution is refined, a behavior that may have similarities with the cancelation observed in the atmospheric heat fluxes by *van Loon* [1979]. This issue has been further discussed by *Bryan* [1986]. Eddy/mean cancelations of the oceanic heat flux have also been found in realistic North Atlantic models by *Bryan and Smith* [1998] and *Smith et al.* [2000].

[4] In contrast with eddy heat transports, meridional eddy salt transports have seldom been analyzed in detail in numerical models. *McCann et al.* [1994] attempted a first estimate of salt transports in a global eddying model, but the results were questionable due to the coarse resolution of the model (0.5°) and the forcing by relaxation to a climatology, at the surface as well as in the deep ocean. Two recent studies have documented the eddy transports of heat and salt (or freshwater) in the Southern Ocean. *Meijers et al.* [2007] have analyzed the horizontal and vertical structure of eddy transports in a $1/8^\circ$ model. *Lee et al.* [2007] have used a global eddy permitting model to diagnose and compare two mechanisms by which eddies affect the mean temperature and salinity fields: the advective effect due to the eddy-induced velocities, and the diffusion of tracers along isopycnals. However, regarding the North Atlantic ocean, we are not aware of any calculation of the eddy fluxes of salt in an eddy resolving model.

[5] *Stammer* [1998] has estimated the eddy salt transport using satellite observations of eddy kinetic energy and a climatology of salinity. Based on a downgradient mixing hypothesis, he computed the salt flux as the product of a lateral mixing coefficient (obtained from the observed surface eddy kinetic energy) and the meridional gradient of salinity averaged over the top 1000 m. This observation-based estimate has never been compared with salt transports from numerical models, although such a comparison would be of interest in order to verify the underlying hypotheses of *Stammer* [1998].

[6] The purpose of the present study is to document the eddy contributions to the meridional transport of salt in the North Atlantic, building on the analyses that have been carried out for the heat transport in eddying ocean models. We use eddy-permitting models at $1/4^\circ$ resolution that have been shown to represent eddy fluxes reasonably well in the Southern Ocean [*Treguier et al.*, 2007] as well as their contribution to interannual variability [*Treguier et al.*, 2010], compared with other models such as *Meijers et al.* [2007] or *Lee et al.* [2007]. However, *Smith et al.* [2000] have demonstrated that a $1/4^\circ$ resolution is not sufficient to resolve key features of the North Atlantic circulation, such as the Gulf Stream separation. Therefore, we also use an eddy resolving model of the North Atlantic at $1/12^\circ$ resolution, and compare the results with the eddy permitting experiments. At a time when the resolution of the ocean in coupled climate models increases, so that these models begin to resolve eddies, it is important to explore how the salt transport depends on model resolution, as was done for the heat transport by *Bryan and Smith* [1998]. We calculate the meridional structure of the eddy salt fluxes and investigate their origin: are the eddy salt fluxes related to the mean gradients, following a simple diffusive model as proposed

by *Stammer* [1998]? Is there compensation between the eddy salt transport and the transport by the time mean flow, as noted in the case of the heat transport by *Cox* [1985] for example?

[7] The following section presents and validates the numerical experiments. In section 3, we describe the model equations for the conservation of volume and salt. We stress that transient eddy correlations do not contribute to the transport of volume, but they do contribute to the transport of salt. This fact motivates our focus on salt rather than freshwater transports. The total, mean and eddy transports of salt are analyzed as a function of latitude, contrasted between the different model experiments, and the degree of eddy/mean cancelation is assessed. Section 4 describes in more details the horizontal and vertical structure the eddy transports of salt, demonstrating that different processes play a role in the North Atlantic depending on the latitude considered, and section 5 summarizes our findings.

2. Numerical Experiments

2.1. Description

[8] The numerical simulations have been performed in the framework of the Drakkar project [*Drakkar Group*, 2007]. The Drakkar group has developed with Mercator-Ocean the global ocean model ORCA025, based on the NEMO modeling framework [*Madec*, 2008]. The ocean model makes the Boussinesq approximation, which means that it conserves volume rather than mass. ORCA025 is based on an isotropic global tripolar grid, with a resolution of $1/4^\circ$ (27 km) at the equator [*Barnier et al.*, 2006]. With this global eddy permitting model, the Drakkar group has performed simulations of the ocean variability over the last 50 years forced by atmospheric reanalyses [*Brodeau et al.*, 2010]. These simulations have been used to address scientific questions regarding the ocean variability at different space and time-scales. In this study we focus on a higher resolution simulation with a $1/12^\circ$ mesh covering the Atlantic ocean and the Nordic seas between 20°S and 80°N (a domain referred to as "NATL", Figure 1). This simulation (hereafter NATL12) is 25 years long, from 1980 to 2004, and is documented in a report [*Treguier*, 2008]. In order to study the effect of model resolution on the eddy fluxes, we also use a NATL025 simulation at $1/4^\circ$ resolution. All simulations are forced by the atmospheric data sets DFS3 or DFS4 (Drakkar Forcing Set 3 or 4) described by *Brodeau et al.* [2010]. The data set is a combination of wind, humidity and air temperature from ECMWF (European Centre for Medium-range Weather Forecasts), together with radiation and precipitation data from other sources [*Large and Yeager*, 2009]. Turbulent air-sea fluxes are computed using bulk formulae from *Large and Yeager* [2009]. The turbulent transfer coefficients are estimated using the difference between the wind velocity and the modeled water velocity. The feedback of ocean currents on the wind stress is important because it modifies the strength of the equatorial upwelling and damps the eddy kinetic energy in eddy-rich regions, as demonstrated by *Eden and Dietze* [2009] in a North Atlantic $1/12^\circ$ model.

[9] As mentioned in the introduction, in a steady state ocean the net meridional transport of salt would be zero. In order to study the relative importance of transport by the eddies and by the time-mean flow, it is very important to use

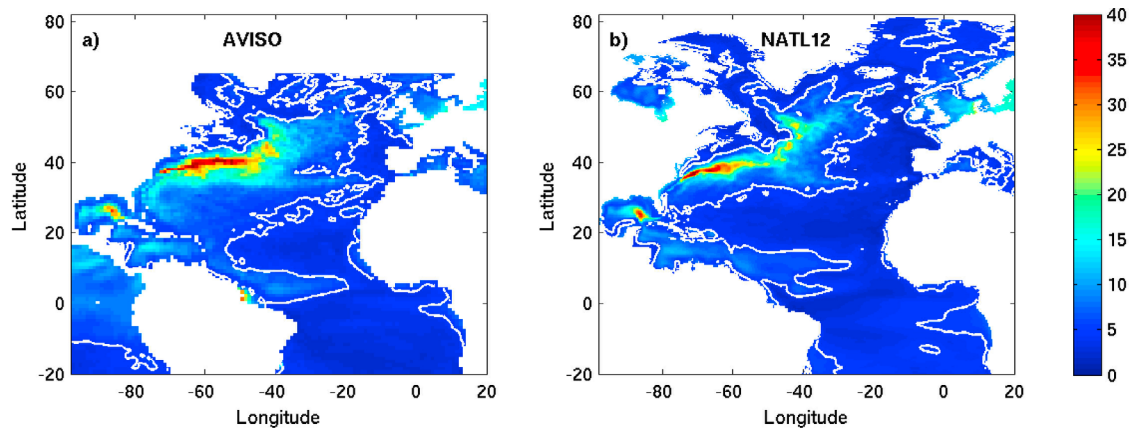


Figure 1. RMS sea level variability (cm) for the period 1993–2004. (a) AVISO data (there is no data north of 65°N due to the presence of sea ice). (b) NATL12. The 5 cm contour is indicated in white.

a numerical simulation that is well equilibrated, with a variability of the salt content of an order of magnitude compatible with observations. It is clearly not the case for simulations carried out for a few decades where the model drift is large. We have run NATL12 for 25 years only due to the cost of such a high resolution model; however, within the Drakkar project, a global ORCA025 simulation has been run recently for 327 years [Penduff *et al.*, 2011] forced by a repeated seasonal cycle computed from the Drakkar Forcing Set DFS4 [Brodeau *et al.*, 2010]. This simulation is used in the present study in order to clarify the role of the model drift and to assess the robustness of our results.

[10] Both regional NATL simulations have been forced at the open boundaries by a monthly climatology built from the global 1/4° simulation ORCA025-G70, which was the best global simulation available in the Drakkar group at the time [Treguier *et al.*, 2007]. This global simulation has been run for a longer period than NATL, from 1958 to 2004. The forcing at the northern and southern boundaries of the NATL domain consists in monthly averages of the velocities, temperature and salinity from ORCA025-G70. A repeated climatological seasonal cycle, built using years 1980–2004 of the global model, has been chosen rather than fully inter-annual boundary conditions in order to focus on the inter-annual variability generated within the NATL domain. At the southern boundary at 20°S, the radiative open boundary algorithm described in Treguier *et al.* [2001] is applied. The northern boundary follows the ORCA tripolar grid around 80°N across the Canadian Archipelago, Fram Strait and the Barents Sea. It is characterized by a shallow bathymetry and very distinct water masses of Arctic origin. If the transport were allowed to vary across this northern boundary as a consequence of the volume conservation imposed over the whole domain, it would generate large fluctuations of freshwater transport, incompatible with observations. In order to avoid this spurious behavior, the properties and velocities of the global model are imposed at the northern boundary, and the conservation of total volume in the domain is ensured at each time step by adjusting the transport at the southern boundary so that the inflow from the boundaries compensates the net loss by evaporation within the domain (which is of the order of 0.35 Sv on average). All the experiments are fully coupled with the sea ice model

LIM of the NEMO modeling framework. For the NATL experiments, a relaxation to the sea ice concentration and thickness of the global ORCA025-G70 run is introduced near the northern boundary to mimic the inflow of arctic ice from into the domain (this is necessary because full open boundary conditions have not been implemented for the ice model yet).

[11] None of the experiments has a fully prognostic Mediterranean sea. The NATL experiments have a closed boundary at 23°E, with a buffer zone to restore temperature and salinity toward the climatology of Levitus *et al.* [1998]. In the long ORCA025 simulation, it has been found necessary to add a three-dimensional restoring to climatology in the Mediterranean Sea, with restoring time of 180 days, to avoid a strong drift in water properties. The need probably arises from the inadequacy of the climatological forcing, since the previous (and shorter) interannually forced ORCA025 experiments produced a useful simulation of the Mediterranean sea [Tsimplis *et al.*, 2008]. There is also restoring in the Gulf of Cadiz in ORCA025 locally, in the Mediterranean water layer only (600–1200 m) with a shorter restoring time (6 days). This local restoring has been removed in NATL12, because the higher resolution together with a local modification of the bathymetry allowed a better representation of the Med water overflow [Treguier *et al.*, 2012]. This special treatment of the Gulf of Cadiz is also omitted in NATL025 for consistency. Besides the restoring in buffer zones and the Mediterranean water, the surface freshwater forcing also includes a restoring to the monthly sea surface salinity climatology of Levitus *et al.* [1998]. The main parameters of the two NATL simulations and the global ORCA025 experiment are summarized in Table 1. Model outputs are 5-days averages. Unless specified otherwise, the results of the NATL configurations presented in this study are averages of these 5-days outputs over a 12-year period, from 1993 to 2004. Results for the long ORCA025 experiment are averaged over the last 27 years because 5-day outputs are available over this period (years 301–327).

2.2. Validation

[12] Figure 1 compares the RMS sea level anomaly measured by altimetry [Duquet *et al.*, 2000] with the RMS sea level anomaly in NATL12. As expected for such a high

Table 1. Characteristics of the Simulations^a

	NATL12	NATL025	ORCA025
Resolution at 45°N	6.5 km	13 km	13 km
Vertical levels	64	46	46
Max horizontal viscosity	$1.25 \cdot 10^{10} \text{ m}^4 \cdot \text{s}^{-1}$	$1.5 \cdot 10^{11} \text{ m}^4 \cdot \text{s}^{-1}$	$1.5 \cdot 10^{11} \text{ m}^4 \cdot \text{s}^{-1}$
Max isopycnal diffusivity	$100 \text{ m}^2 \cdot \text{s}^{-1}$	$300 \text{ m}^2 \cdot \text{s}^{-1}$	$300 \text{ m}^2 \cdot \text{s}^{-1}$
Surface salinity restoring for 10 m depth	176 days	60 days	60 days
Forcing set	DFS3	DFS4	DFS4 clim

^aFor clear reference, NATL12, NATL025 and ORCA025 are the simulations documented as NATL12-BAMT20, NATL025-BRD80 and ORCA025-MJM01 in the Drakkar simulation ensemble, respectively. The main difference between the high resolution ($1/12^\circ$) and the low resolution ($1/4^\circ$) experiments is the horizontal viscosity (biharmonic, maximum at the equator, varying as the third power of the grid size) and the isopycnal diffusivity (Laplacian, maximum at the equator, proportional to the grid size). The Drakkar forcing sets DFS3 and DFS4 are described in *Brodeau et al.* [2010].

resolution model, the agreement is good. The model reproduces the main eddy regions (Loop current in the Gulf of Mexico, Gulf Stream, Azores front, North Atlantic Drift) with a level of variability compatible with observations. In the $1/4^\circ$ model the eddy energy is underestimated and the path of the mean currents differs more from observations (not shown); this sensitivity to model resolution has been described by *Smith et al.* [2000] using the POP model (Parallel Ocean Program).

[13] We have compared the evolution of the salinity in the three models. The time series of the domain-averaged salinity is dominated by a trend which is smaller in ORCA025 but of the same order of magnitude as in the short experiments: over 25 years, the mean salinity in the whole NATL domain increases by 0.001 PSU in ORCA025, by 0.003 PSU in NATL12, and decreases by 0.009 PSU in NATL025. However, this small trend integrated over the whole NATL domain hides large opposing trends in the subtropical and the subpolar gyres in the short experiments. Figure 2 contrasts the trends in these two basins in the three models; the drift is much reduced in the long ORCA025 simulation compared with the short NATL experiments. The drift in the gyres in NATL is larger in amplitude than changes typically observed in the ocean over a few decades (for example, *Curry et al.* [2003] find that the averaged salinity of the North Atlantic between 40°N and 60°N decreased by 0.03 PSU over 30 years). The model drift is an adjustment problem, and not a response to the interannually varying forcing, as has been verified by cycling over the 50 years of the DFS4 atmospheric forcing twice with the

ORCA025 model [*Treguier et al.*, 2010; *Grist et al.*, 2010]: the drift was much reduced during the second 50-years long experiment. From Figure 2 one can further note that in the NATL domain, the initial drift shows no simple dependency on model resolution. In the subpolar gyre the salinization is larger in NATL12 compared with NATL025, but in the subtropical gyre the freshening is larger in NATL025. *Rattan et al.* [2010] have performed a detailed analysis of these initial drifts in the $1/4^\circ$ models, focused on the Labrador Sea. They have found that the interpretation is complex as the drifts result from an interplay between errors in the model, its initial conditions and its forcing field.

[14] As an additional validation of our models, the meridional advective heat transport (MAHT) is presented in Figure 3 for our three simulations, for comparison with results of the POP North Atlantic model at increasing resolutions of 0.4 , 0.2 and 0.1° , first published by *Bryan and Smith* [1998] (the same figure appears in *Hecht and Smith* [2008]). In our case the transports are estimated across the model grid lines, which are not exactly parallel to lines of constant latitude north of 20°N , but the small difference does not affect the results significantly at the latitudes considered here.

[15] The model MAHT can be compared with the recent estimate of *Large and Yeager* [2009] derived from surface fluxes, also indicated in Figure 3. *Large and Yeager* [2009] compute the meridional heat transport by integrating the surface air-sea heat flux divergence, starting from zero at the north pole. The light pink shading in Figure 3 represents the range of their annual mean estimates over the years

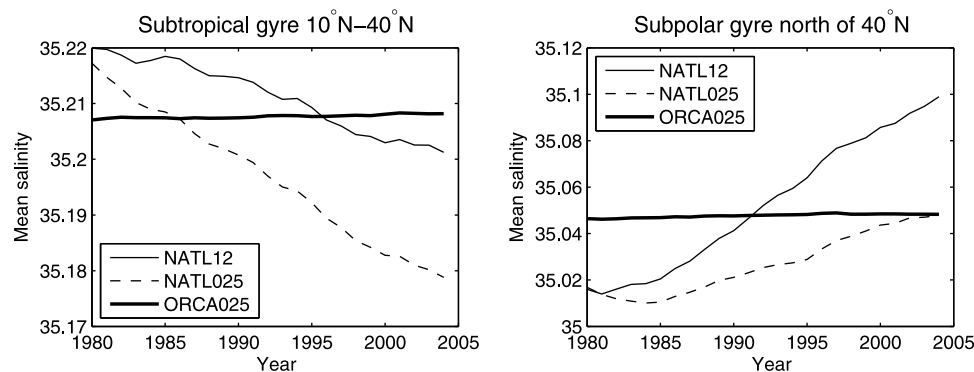


Figure 2. Time series of averaged salinity in the three models. For ORCA025, the last 25 years of the climatological run are plotted. (left) Subtropical gyre between 10°N and 40°N ; (right) subpolar gyre north of 40°N .

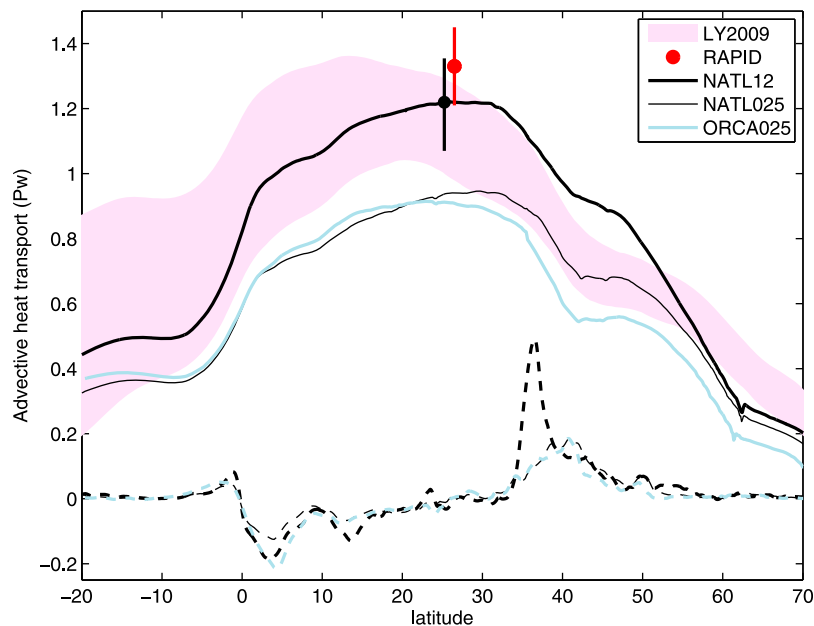


Figure 3. Meridional heat transport, averaged over years 1993–2004 for the NATL models and over the last 27 years of the ORCA025 climatological experiment. Solid lines indicate the total transport and dashed lines the eddy contribution. For NATL12, a black vertical bar indicates the range of annual mean heat transport values between 1993 and 2004, at the latitude where the maximum annual value is found (25.25°N). The pink shading indicates the range of annual mean transport estimates over the years 1984–2006, computed by *Large and Yeager* [2009] from air-sea surface fluxes. The red dot marks the heat transport across the RAPID array (with its range of uncertainty) from *Johns et al.* [2011].

1984–2006. NATL12 agrees the best with these data, excepted for its large heat transport between 40°N and 50°N. The range of annual mean transports for NATL12 at 25.25°N (where the maximum is found) is indicated by a black bar, showing that the amplitude of the interannual variability is in agreement with *Large and Yeager* [2009]. At 26.5°N, the MAHT has recently been estimated with unprecedented accuracy using the RAPID array [*Johns et al.*, 2011]. Their value of the MAHT (1.33 ± 0.12 Pw) is indicated in red in Figure 3. It is larger than *Large and Yeager* [2009] and also larger than most previous estimates. Among our models, only NATL12 is compatible with this new observation at 26.5°N.

[16] The dependency on model resolution is very clear in Figure 3, because the two 1/4° models are closer to each other than to the 1/12° model, even though NATL025 and ORCA025 have different boundary conditions (ORCA025 being a global model) and different forcing fields (NATL025 has an interannual forcing, ORCA025 a climatological forcing). The divergence of the meridional heat transport (advective and diffusive) is balanced by the surface heat flux, and the trends of the heat content. The increase of the MAHT from NATL025 to NATL12 is consistent with the increase of the integral of the surface flux (not shown); more heat advected northward in NATL12 results in a greater heat loss to the atmosphere. This is expected within a forced ocean model, where the air temperature is imposed and the air-sea heat flux is calculated by bulk formulae.

[17] Just as noted by *Bryan and Smith* [1998], the difference between the MAHT at 1/4° and 1/12° is due to changes in the mean transport (e.g., a stronger Gulf Stream and North Atlantic current) rather than being due to changes in the

eddy component, which is generally small compared to the total MAHT (dashed lines in Figure 3). The general shape and amplitude of the eddy advective heat flux is similar in all three Drakkar models, and also similar with the POP model. Overall, in agreement with a classical downgradient mixing hypothesis, eddies flux heat out of the subtropical gyre, with maxima of southward eddy heat flux at the southern boundary of the subtropical region (5°N to 15°N) and a maximum of northward eddy heat transport around 35°N to 40°N at the limit between the subtropical and the subpolar region. In all models, eddy heat fluxes are small in the subpolar gyre. The large peak in eddy heat transport (0.4 PW) found at 36°N in NATL12 is a special feature of this model, not found in POP. It is completely compensated by a corresponding drop in the heat transport by the time-mean flow, so that it has no effect on the total heat transport (Figure 3). This feature is further discussed in section 4.

3. Freshwater, Volume and Salt Transports

3.1. Rationale

[18] Meridional transports of salt are difficult to estimate from data, due to the lack of adequate observations of ocean velocities. The uncertainty of the total volume transport across a section is usually of the order of—or larger than—the total transport itself. For this reason, oceanographers have focused on the transport of freshwater, as explained for example by *Wijffels* [2001]. Freshwater is defined as

$$\frac{S_0 - S}{S_0}, \quad (1)$$

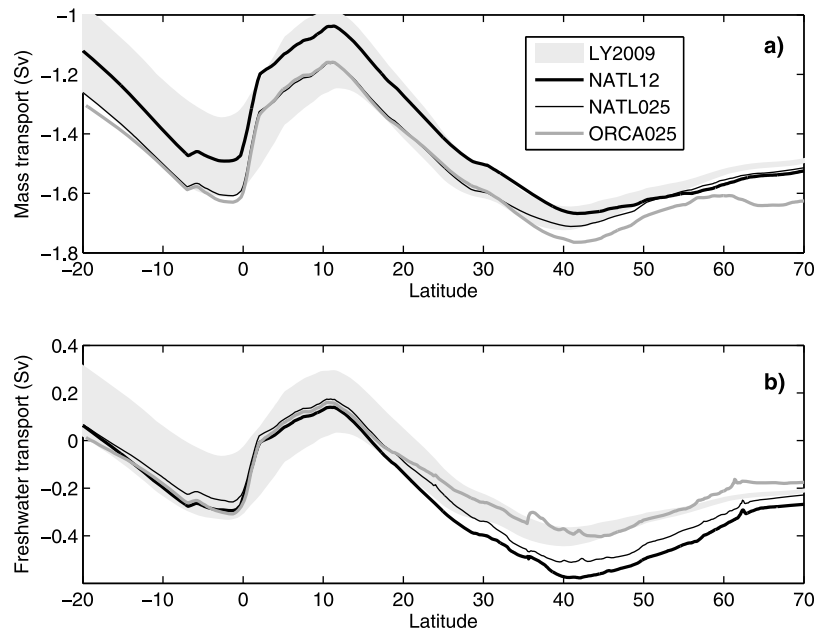


Figure 4. (a) Meridional volume transport and (b) freshwater transport, averaged over years 1993–2004 for the NATL models and over the last 27 years of the ORCA025 climatological experiment. The grey shading is based on the range of annual mean transport estimates over the years 1984–2006, computed by *Large and Yeager* [2009] from air-sea surface fluxes. *Large and Yeager* [2009] do not take into account the transport through Bering Strait; a fixed value of -1.4 Sv (Figure 4a) and -0.12 Sv (Figure 4b) has been added to their freshwater transport to allow comparison with the models.

S being the salinity and S_0 a reference salinity. The equation for the freshwater content is obtained by combining the conservation equations for volume and salt. When S_0 is defined as the averaged salinity along a section, the freshwater transport across that section is independent of the total mass (or volume) transport. Even when an arbitrary reference salinity is used [*Talley*, 2008], the correlation of velocity and salinity errors ensures that the freshwater transport can be determined with some skill despite the unknown total volume transport [*Ganachaud and Wunsch*, 2003].

[19] In a numerical model where the mass transport is known exactly, it is possible to consider both volume and salt transport separately. Let us assume an ocean volume \mathcal{V} delimited by a boundary b (say, two meridional sections across a basin) and an air-sea interface of surface s . The model we use makes the Boussinesq approximation, so that the mass conservation reduces to the conservation of volume

$$\iint_s \frac{\partial \eta}{\partial t} + \oint_b v = - \iint_s F_w, \quad (2)$$

where v is the velocity normal to the boundary, η is the free surface elevation and F_w is the freshwater forcing at the air-sea interface. In our model $F_w = E - P - R + F_w^*$, where $E - P - R$ is the balance of evaporation minus precipitation and runoffs, and F_w^* is the restoring to the climatological sea surface salinity of *Levitus et al.* [1998]. Equation (2) is linear; when variables are split into a time-mean and a fluctuating (eddy) part, and averaged in time, no eddy effect appears.

[20] The conservation equation for salt content, on the other hand, is impacted by eddy fluxes. Our model uses the

linear free surface formulation of *Roulet and Madec* [2000]. The free surface equation is

$$\frac{\partial \eta}{\partial t} = w(z=0) - F_w, \quad (3)$$

where w is the vertical velocity. The salinity equation is

$$\frac{\partial S}{\partial t} = -\nabla(\mathbf{u}S) + \nabla(F_D) + \delta(z=\eta)S(F_w + F_i), \quad (4)$$

where \mathbf{u} is the three-dimensional velocity, F_D is the diffusive flux, and F_i is the surface ice-ocean flux and δ the Dirac operator. F_w is the concentration-dilution flux also appearing in (2) which contributes to the evolution of salinity. This equation is similar to the tracer equation 1b in *Roulet and Madec* [2000], excepted that the net tracer flux F_{ext} is zero in our case because evaporation, precipitation and runoff are assumed to carry no salt: there is no salt exchanged through the surface of the ocean. Equation (4) can be integrated vertically to derive the equation for the conservation of salt in a fluid column

$$\int_{-H}^{\eta} \frac{\partial S}{\partial t} = -\nabla_h \int_{-H}^{\eta} \mathbf{u}_h S + \int_{-H}^{\eta} \nabla(F_D) + \delta(z=\eta)SF_i, \quad (5)$$

where \mathbf{u}_h is the horizontal velocity and ∇_h the horizontal divergence operator. The surface water flux F_w does not enter (5) because the concentration/dilution effect in (4) is canceled by the vertical advection of salt wS at $z=0$, with $w(z=0)$ being given by (3). This ensures a very good global conservation of salt [*Roulet and Madec*, 2000], consistent with the fact that no salt is exchanged with the

Table 2. Surface Water Flux, Positive for Net Evaporation, Over the Whole NATL Domain and in Three Latitude Bands Representing the Subpolar, Subtropical and Tropical Regions, Respectively^a

	NATL12	NATL025	ORCA025
NATL total upward water flux (Sv)	0.41 (0.04)	0.26 (0.06)	0.34 (0.05)
North of 40°N	-0.14 (-0.01)	-0.20 (0.03)	-0.11 (0.09)
Between 10°N and 40°N	0.61 (0.05)	0.53 (0.06)	0.56 (0.05)
Between 0° and 10°N	-0.39 (0.01)	-0.4 (0.01)	-0.43 (-0.01)
NATL total ice/ocean flux (Sv)	-0.09	-0.07	-0.14

^aThe net F_w is indicated, with the restoring component of the flux F_w^* given in parentheses (Sv). The ice-ocean flux results from net ice melt in the NATL domain.

atmosphere at the surface. In our model, as a consequence of the linearized free surface formulation, the lateral fluxes at the boundaries are integrated vertically from the bottom $z = -H$ to the fixed depth $z = 0$ (neglecting the sea surface elevation η). However, the variation of volume due to the motion of the upper boundary η cannot be neglected in the global model

$$\frac{\partial}{\partial t} \int_{-H}^{\eta} S = \int_{-H}^{\eta} \frac{\partial \bar{S}}{\partial t} + S \frac{\partial \eta}{\partial t}. \quad (6)$$

In the North Atlantic models, the volume is kept constant by adjusting the flow at the southern open boundary, so that $\partial \eta / \partial t = 0$ when integrated over the domain.

[21] When the salinity S and velocity v are decomposed into a mean and eddy part ($S = \bar{S} + S'$ and $v = \bar{v} + v'$), the salt conservation in a volume \mathcal{V} , averaged in time, can be expressed as

$$\frac{\partial}{\partial t} \iiint_{\mathcal{V}} S + \oint_b \bar{v} \bar{S} + \oint_b \bar{v}' S' + \oint_b \bar{F}_D = \iint_s \bar{F}_i, \quad (7)$$

where F_D is the diffusive flux of salt (due to the model parameterized isopycnal mixing). When volume \mathcal{V} is our North Atlantic domain, (7) shows that the salt content can vary through advection or diffusion of salt in the ocean at the open boundaries, or through the surface ice-ocean flux. The latter has a net freshening effect because sea ice is advected into the North Atlantic from the Nordic Seas and melts there. Note that when the parameterized diffusive flux F_D is small (which is the case in a high resolution eddy resolving model), outside the ice-covered regions, and if the salt content is at equilibrium, (7) reduces to

$$\oint_b \bar{v} \bar{S} + \oint_b \bar{v}' S' = 0, \quad (8)$$

the eddy transport of salt is exactly compensated by the mean, so that the total advective transport into the domain is zero (in the case of the North Atlantic, it means that the net meridional transport is non-divergent, independent of latitude).

[22] An equation for the conservation of freshwater defined by (1) is readily obtained by subtracting (7) divided by a reference salinity S_0 from the mass conservation (2). However, in a numerical model volume and salt fluxes can be analyzed separately and it makes sense dynamically. The

ocean volume adjusts through fast dynamics. A localized volume flux forces gravity waves; persisting anomalies of $(E - P - R)$ give rise to responses referred to as Goldsbrough-Stommel gyres [Huang and Schmitt, 1993], which are fast ocean responses set up by barotropic Rossby waves. On the other hand, the salt content evolves on very long timescales when the net salt transport into a region is non-zero (timescales of centuries, typical of the world ocean thermohaline circulation). The variability of the freshwater (1) is thus potentially complex, as it combines these very different timescales.

3.2. Volume and Freshwater Transport

[23] The net meridional volume transport is shown in Figure 4a for the three experiments. In all cases, it is exactly balanced by the surface flux F_w , because our numerical model conserves volume exactly. The inflow at the northern boundary is rather large (1.5 to 1.6 Sv). It results from the water balance of the Arctic in the global 1/4° model, which has been studied in detail by Lique *et al.* [2009]. Our global model overestimates the transport through Bering Strait: 1.3 Sv in the simulation ORCA025-G70 used as boundary condition for the NATL domain, and 1.4 Sv in the climatological ORCA025 simulation. These values are larger than the recent observation of 0.8 Sv by Woodgate and Aagaard [2005].

[24] The amplitude of the volume transport is in very good agreement with the estimates of Large and Yeager [2009] reproduced in Figure 4. Starting from the north, the transports in Figure 4 first increase southward up to 40°N due to the net freshwater input in the subpolar gyre, then decrease due to evaporation in the subtropical gyre, and increase again in the tropics. The net surface water flux in these three latitude bands is indicated in Table 2, together with the restoring term F_w^* . The contribution of restoring to the surface fluxes is small, although non negligible.

[25] Our model results demonstrate that like the meridional heat transport, the volume transport is sensitive to the model resolution. The subpolar freshwater gain is smaller in NATL12 compared with NATL025 and the subtropical loss is larger, resulting in differences in meridional volume transport of about 0.1 Sv between the two experiments. The differences in both gyres result from the stronger evaporation in the high resolution model (precipitation and runoff are prescribed and identical in both models); this stronger evaporation is consistent with the larger northward heat transport in NATL12 discussed in the previous section. The difference is not due to the relaxation to observed sea surface salinity which is relatively small (Table 2). Over most of the domain the restoring term contributes to attenuate the differences between the two NATL models at different resolutions.

[26] The corresponding transports of freshwater are plotted in Figure 4b (note that two different offsets at 70°N are applied to plot the Large and Yeager [2009] transport in Figures 4a and 4b). We have chosen $S_0 = 34.8$ in (1); freshwater transports computed with reference salinities between 34.8 and 35 are barely distinguishable from each other on the scale of Figure 4 (not shown). The latitudinal variations in freshwater transports are different from those of the volume transport, demonstrating that the net advective

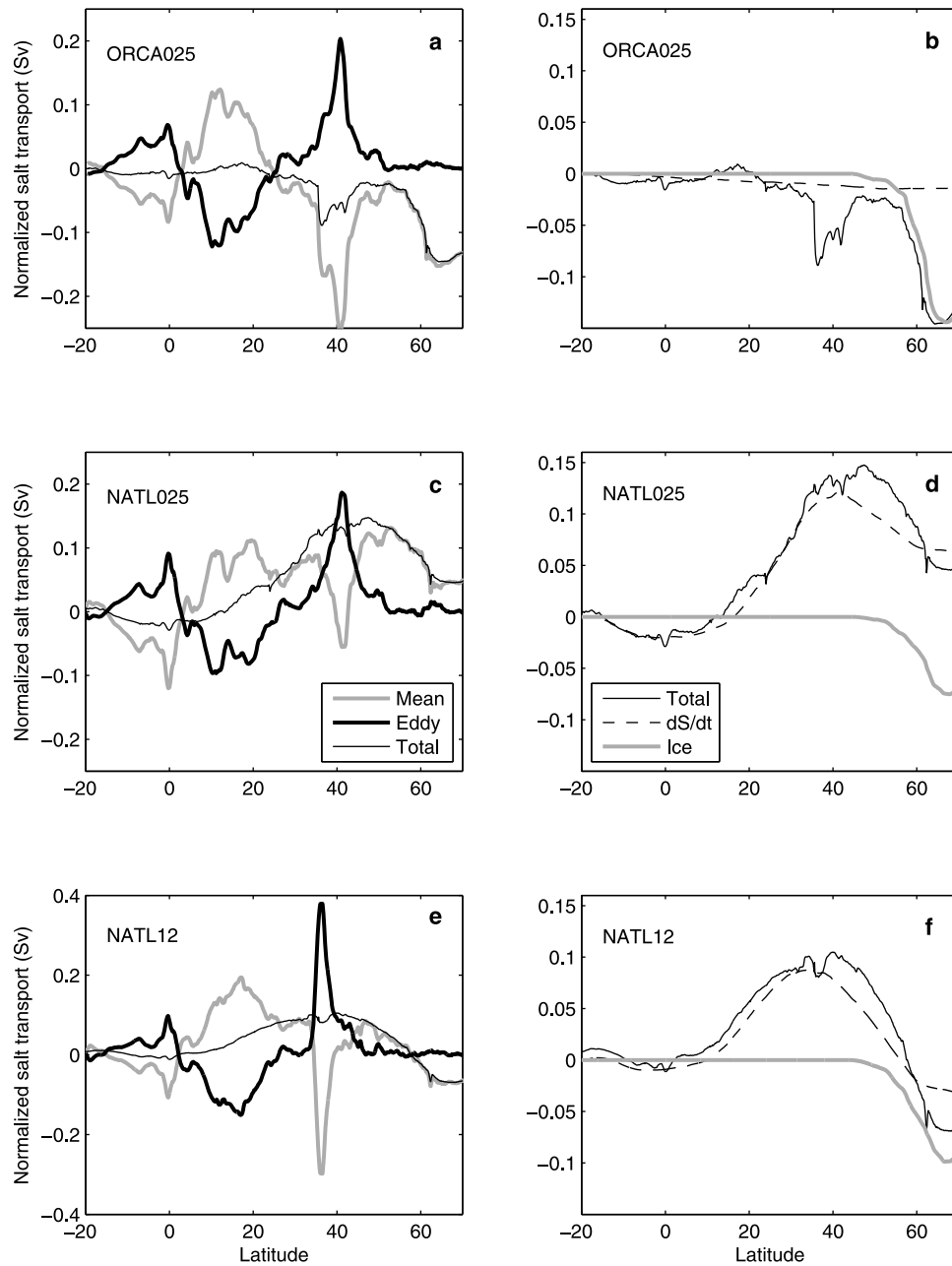


Figure 5. Variations with latitude of the meridional salt transport, averaged over years 1993–2004 for the NATL models and over the last 27 years of the ORCA025 climatological experiment. (a, c, and e) Mean, eddy and total meridional salt transports (the mean and total are plotted as an anomaly relative to the total transport at 20°S, which is -1.3 Sv in ORCA025 and NATL025 and -1.2 Sv in NATL12). (b, d, and f) Comparison of the total transport with the salt content variation and the integral of the ice-ocean flux in the three model experiments.

transport of salt is not zero in the models. For example, the decrease in freshwater transport from 15°N to 40°N is larger in the North Atlantic models than in the global model, and the latter is the most compatible with the surface fluxes of *Large and Yeager* [2009]. These differences will be analyzed further in the next section by concentrating on the transport of salt, which we compute in units of Sverdrups ($10^6 \text{ m}^3 \cdot \text{s}^{-1}$), normalized by a constant salinity S_0 . Throughout this paper

we choose $S_0 = 34.8$; this value is arbitrary and used only to help the reader compare the relative contribution of the volume flux and the salt flux to the freshwater (1).

3.3. Salt Transport

[27] The time-averaged meridional advective salt transport (normalized by S_0), which is the difference between the curves in Figures 4a and 4b, can be decomposed into its mean and eddy component (Figure 5). In order to focus on

the meridional structure within the domain, the total transport at the southern boundary of the NATL domain is subtracted for each model (see the caption of Figure 5). The first thing to note is that the eddy transports are significant: across the subtropical gyre, the eddy salt transport divergence is larger than 0.2 Sv, which is not small compared to the evaporation-precipitation balance over the area (0.6 Sv, see Table 2). A second very striking characteristic is the compensation between eddy and mean salt transport. In the global experiment ORCA025 (Figure 5a) the compensation is almost perfect, the total salt transport (thin black line) being small, excepted between 36°N and 40°N, and north of 60°N. Figure 5b shows again this total salt transport for ORCA025, compared with other terms in the conservation equation (7): the integral of the salt content drift (dashed line) is very small because the model has been run for more than 300 years. As shown by (6) it is the sum of two terms: the salinity increase in the fixed volume delimited by a constant surface $z = 0$, and the contribution of the variation in the sea surface elevation. Over the last 25 years of ORCA025, the respective contribution of these two terms is 0.009 Sv and 0.004 Sv. The contribution from the ice-ocean flux (thick grey line) explains entirely the transport north of 60°N. The rapid increase of the southward transport at 36°N is probably balanced in the model by the relaxation of salinity (and temperature) to observed water mass properties in the Mediterranean Sea and the Gulf of Cadiz. Near 40°N the diffusion of salt (parameterized by an isopycnal Laplacian operator) may be significant at the boundary between the subtropical and the subpolar gyre, and can also contribute to balance the nonzero advective salt transport. These terms have not been saved in the model archive and are difficult to recompute with enough precision to verify the balance.

[28] In NATL025 (Figure 5d) and NATL12 (Figure 5f), the total salt transport is larger than in ORCA025, and it is mainly balanced by the drift of the salt content. Note that the ice-ocean flux is smaller in the NATL experiments than in ORCA025, because some parameters for the sea ice model were different in the climatological ORCA025 run. The sea ice flux in the North Atlantic can be compared with the sea ice export from the Arctic Ocean through Fram Strait, which is around 0.09 Sv [Dickson *et al.*, 2007]. In both regional and global simulations, Figure 5 demonstrates the strong compensation between eddy and mean advective meridional salt fluxes. The key result is that in a well equilibrated eddy model, the required cancelation of the salt convergence is realized because eddies compensate mean flow advection at each latitude, both eddy and mean fluxes being large (of the same order of magnitude as the evaporation/precipitation balance). The lateral diffusion parameterized in the eddy models (in our case, an isopycnal Laplacian diffusion) does not play a significant role in the basin-wide meridional transports, even at 1/4°.

[29] Let us now consider the meridional structure of the eddy salt fluxes. The variations as a function of latitude are quite similar in the three experiments with a maximum near 36–40°N, a minimum near 15°N, and a maximum just north of the equator. In all models, the eddy salt fluxes are small in the subpolar gyre. The amplitude of the eddy transport of

salt increases with the model resolution, from 1/4–1/12°, as the spectrum of eddy variability is better represented in the model. A strong sensitivity to resolution appears at the latitude of the Gulf Stream separation (36°N), with a much larger eddy salt flux in NATL12 compared with the 1/4° models. In these respects, the salt transport behaves like the heat transport described in section 2.

[30] Most of the $\overline{v'S'}$ correlation is due to variability at timescales typical of oceanic eddies, and shorter than one year. This is confirmed by comparing the eddy salt transport averaged over the 1993–2004 period with averages over individual years for NATL12 (Figure 6a). Although there is year-to-year variability, the overall meridional structure of the eddy salt transport is well established using only one year of model output. We have also estimated the part of the $\overline{v'S'}$ correlation that results entirely from the seasonal cycle. To do this, we have computed an average seasonal cycle over the 12 years 1993–2004. The 12 monthly values of velocity and salinity, \bar{v} and \bar{S} are used to compute a salt transport $\bar{v}\bar{S}$. The difference with the transport by the mean flow $\bar{v}\bar{S}$ is the contribution of the seasonal cycle, represented by a thin line in Figure 6a. This contribution is small, excepted in the tropics. Between the equator and 10°N the seasonal cycle explains half the eddy transport of salt in NATL12. This seasonal contribution is complex to analyze because it is the sum of large and opposite northward and southward fluxes depending on longitude; at 10°N where the seasonal eddy flux is maximum in amplitude, the seasonal cycle at the western boundary plays the most important role (not shown).

[31] In the subtropical gyre, the meridional structure of the eddy salt fluxes appears in good agreement with the one computed by Stammer [1998] based on a simple down-gradient mixing hypothesis. Using the meridional gradient of salinity averaged over the top 1000 m, he found a maximum eddy salt transport near 40°N and a minimum near 10°N (his Figure 8b). We compare in Figure 6b the eddy salt transport in NATL12 and a similar estimate based on the gradient of the averaged salinity in the top 500 m, and a constant mixing coefficient κ . Figure 6b shows a calculation based on the model salinity gradient and a calculation based on the observed salinity climatology of Levitus *et al.* [1998]: both give similar results. The mixing coefficient we have chosen, $\kappa = 250 \text{ m}^2 \cdot \text{s}^{-2}$, is similar to the averaged κ found by Stammer [1998] in the subtropical gyre (he obtained larger values in the western boundary current system). We have used a depth of 500 m to average the salinity gradient rather than 1000 m like Stammer [1998] because it fits better the model estimate. When salinity is considered over the top 1000 m, a larger salinity gradient appears around 30–35°N due to the Mediterranean water while there is no enhanced southward eddy salt transport in NATL12 in that latitude band. In summary, Figure 6b seems to validate the down-gradient hypothesis near 15°N, but less so in the 36–40°N band where the peak of eddy transport in the model does not correspond to the latitude of the maximum salinity gradient. Figures 5 and 6 suggest that the main role of eddy salt fluxes is to mix salt out of the subtropical gyre, in order to compensate for the input of salt into the gyre by mean advection, which is itself partly due to the volume flux convergence

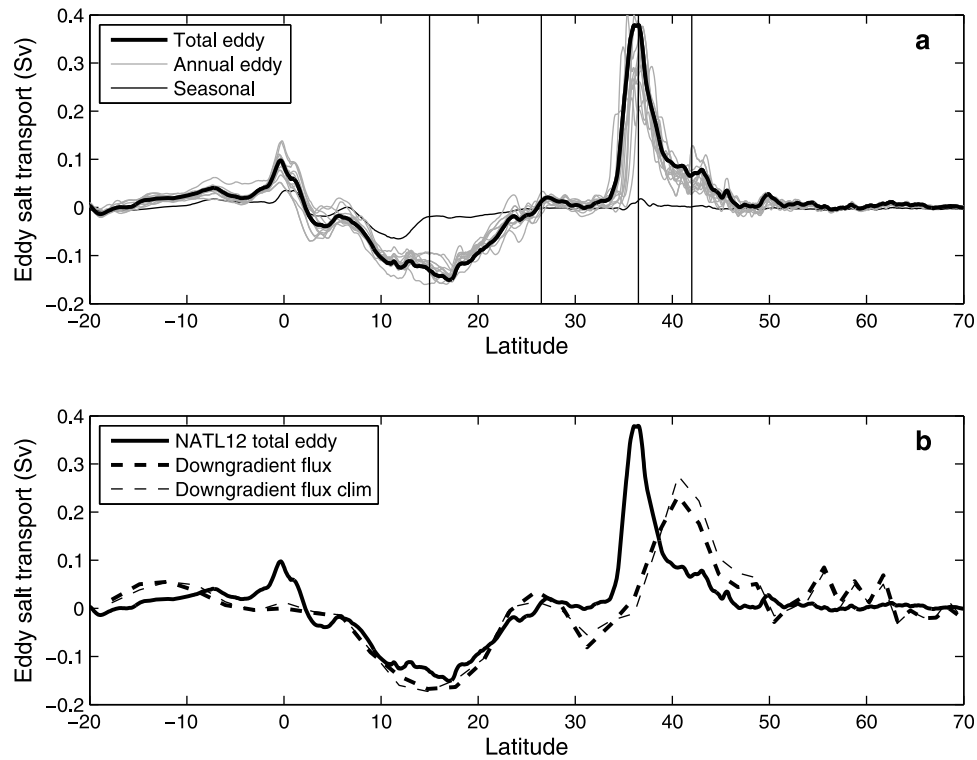


Figure 6. (a) Meridional eddy salt transport for NATL12 experiment over the 1993–2004 period, compared with estimates for each individual year (grey lines) and the contribution of seasonal $v'S'$ correlations (thin black line). Four latitudes are marked where the salt transport is examined in more detail in Figure 7. (b) Comparison of the NATL12 eddy salt transport with an estimate using a constant mixing coefficient $\kappa = 250 \text{ m}^2 \cdot \text{s}^{-2}$ and the meridional gradient of salinity in the top 500 m, for the NATL12 model (thick dashed line) as well as the Levitus climatology (thin dashed line).

driven by the excess evaporation. In order to go beyond this simple picture, an examination of the zonal and vertical structure of eddy salt fluxes in the subtropical gyre as well as an estimation of their advective and diffusive components is presented in the following section.

4. Structure and Origin of Eddy Salt Fluxes

[32] Figure 7 represents the eddy salt flux cumulated from the west in the NATL12 and NATL025 models, at four latitudes. For NATL12, these latitudes, indicated in the top map of Figure 7, correspond respectively to the minimum and maximum eddy salt transport (15°N and 36.5°N , see Figure 6), the maximum sea surface salinity (26.5°N) and the northern boundary of the gyre (42°N), where the strength of the eddy salt transport is similar to 15°N but with an opposite sign. The cumulated transport at 42°N in Figure 7 displays a strong eddy contribution at the longitude of the Gulf Stream/North Atlantic Current system, but eddy fluxes exist all along the section. At the latitude where the northward eddy salt flux is maximum in NATL12 (36.5°N) almost all the eddy flux occurs at the western boundary. In the center of the gyre at 26.5°N , the eddy salt flux is very small outside the Gulf of Mexico. This is consistent with Stammer's [1998] diffusive flux hypothesis, since this latitude (which is the latitude of the RAPID array) corresponds to the salinity maximum of the subtropical gyre, where meridional gradients of salt are small. Near the southern

boundary of the gyre, at 15°N , where the maximum southward eddy salt transport is found, the eddy contribution is significant at all longitudes, with no large contribution from either the western or the eastern boundary.

[33] The contribution of different layers to the total eddy salt flux is presented in Figure 8 for the four latitudes 15°N , 26.5°N , 36.5°N and 42°N . The basin-wide flux is dominated by contributions from the upper layers above the thermocline, explaining why it is better to average the meridional gradients over the top 500 m (our Figure 6) rather than 1000 m [Stammer, 1998] when attempting to estimate fluxes from gradients. The complex vertical structure at 15°N , with a surface minimum, is explained by the contribution to the zonal integral of the Caribbean Sea (not shown), where the surface eddy salt flux is northward contrary to the Atlantic basin at this latitude. This may be a model artifact, as the surface meridional gradient of salt is reversed and overestimated there in the model due to an invasion of anomalously fresh waters from the Amazon and Orinoco rivers. This problem may be related to the values we have chosen for the river run-off, a climatology from Dai and Trenberth [2002], or to errors in the model circulation or vertical mixing near the river mouths. The vertical and longitudinal structure of the eddy salt flux is similar in the $1/4^\circ$ model and the $1/12^\circ$ model, although large differences can exist at a given latitude as demonstrated by Figures 7 and 8. At 36.5°N the eddy salt flux is small in NATL025 because the Gulf Stream separation occurs too far north. The larger eddy

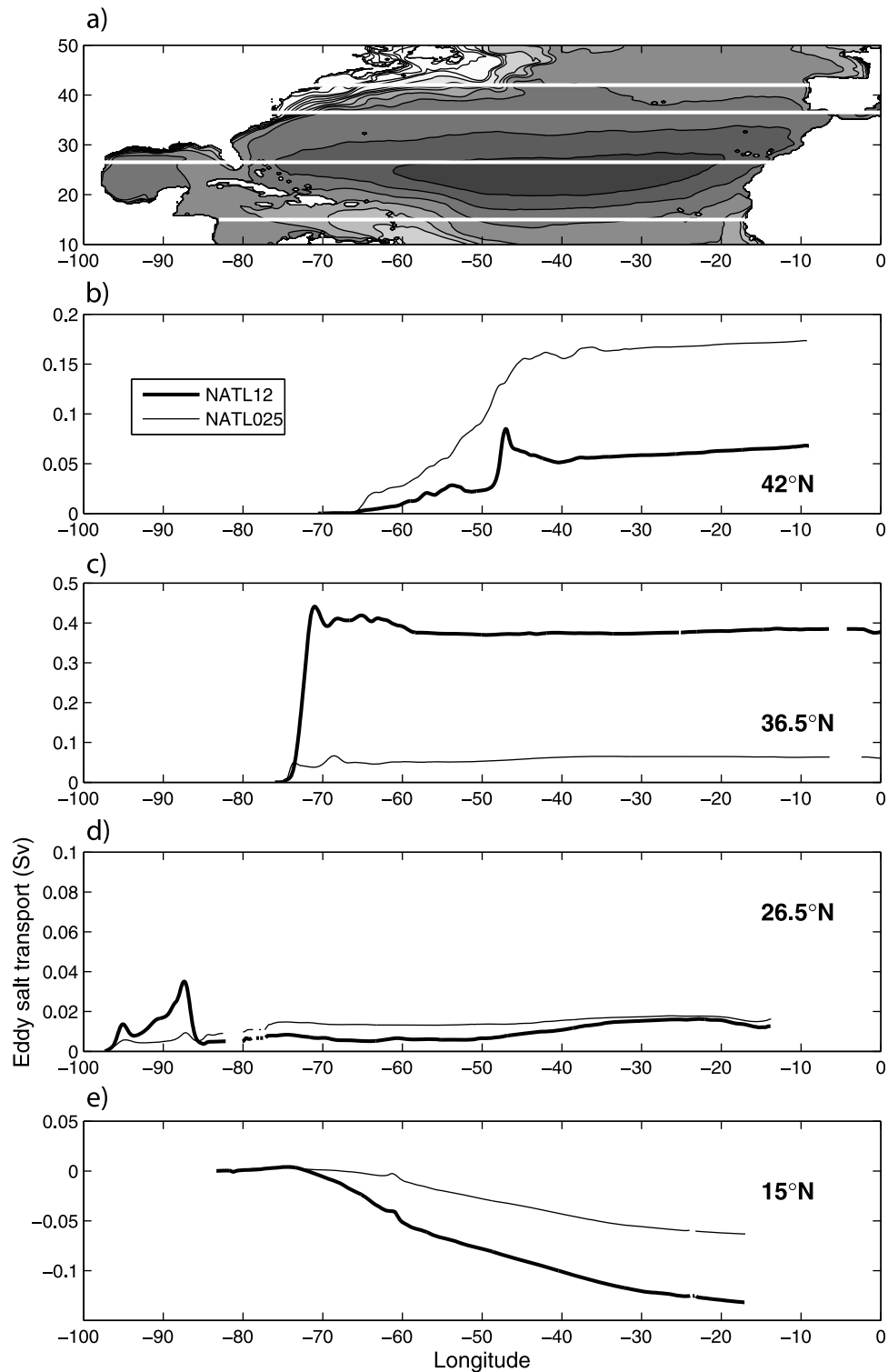


Figure 7. (a) Map of mean sea surface salinity in NATL12 (contour interval 0.5 PSU, more saline waters are indicated by a darker grey, maximum contour is 37 PSU). (b–e) Meridional eddy salt transport for the NATL12 and NATL025 experiments over the 1993–2004 period, cumulated from the west at the four latitude lines indicated in the top map.

variability in NATL025 compared with NATL12 at 42°N results from this shift in the Gulf Stream path.

[34] The contrasting longitudinal structure of eddy fluxes at 36.5°N and 15°N in Figure 7 deserves attention, but first it

is important to establish its significance. The equation for the conservation of salt (4) shows that it is only the *divergence* of the advective fluxes that impacts the mean salinity locally, but eddy fluxes often have a large *rotational* component

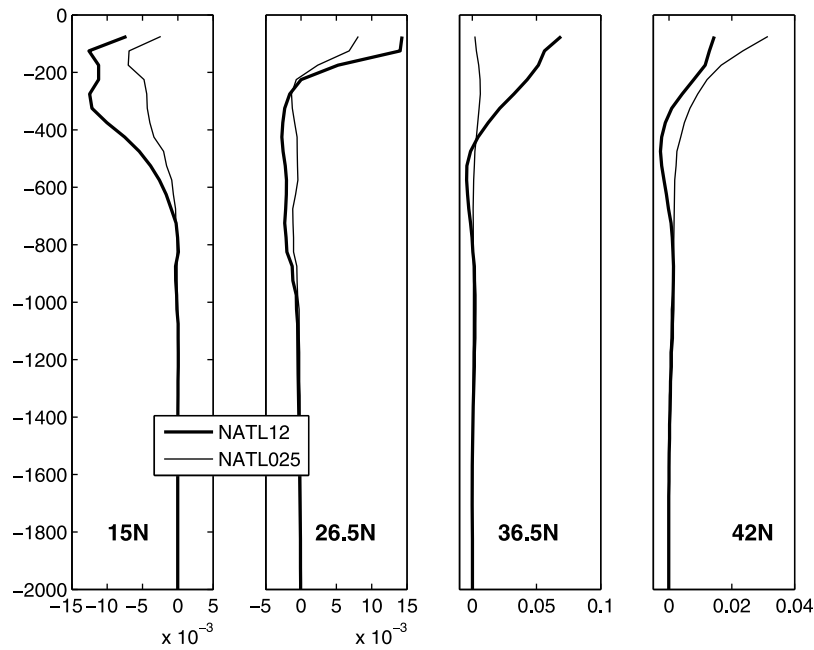


Figure 8. Contribution to the basin-wide and vertically integrated eddy salt flux (in Sv), in 50 m depth bins, as a function of depth.

which makes their effect on the mean flows difficult to diagnose. Different methods have been proposed to remove the rotational component [e.g., *Eden et al., 2007*]. However, these methods are subject to arbitrary choices regarding lateral boundary conditions [*Fox-Kemper et al., 2003*]. These authors point out that the local effect of eddy fluxes over a region of interest can be evaluated by computing the integral of the eddy flux divergence over the area, a quantity that is independent of the rotational component of the eddy

flux. Following *Fox-Kemper et al. [2003]* we have plotted in Figure 9 the sum of the divergence of the eddy salt flux between two latitudes, cumulated from the west, for the high resolution NATL12 model. We have verified that the total integral across the basin is equal to the difference between the eddy salt transports at these two latitudes (the numerical model conserves salt to machine accuracy); this can also be verified by comparison of the cumulated values in Figure 9 with Figure 6. The latitude 36.5°N corresponds to the

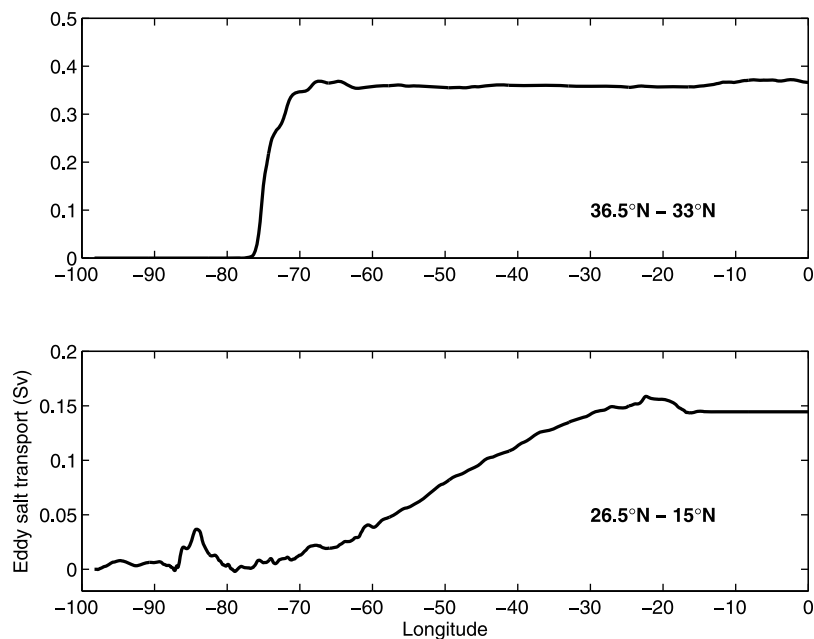


Figure 9. Divergence of the eddy salt flux normalized by S_0 in NATL12, integrated meridionally between two latitudes and cumulated zonally from the west boundary. The total cumulated values across the basin (Sv) is the difference between the total eddy salt flux at the two latitudes.

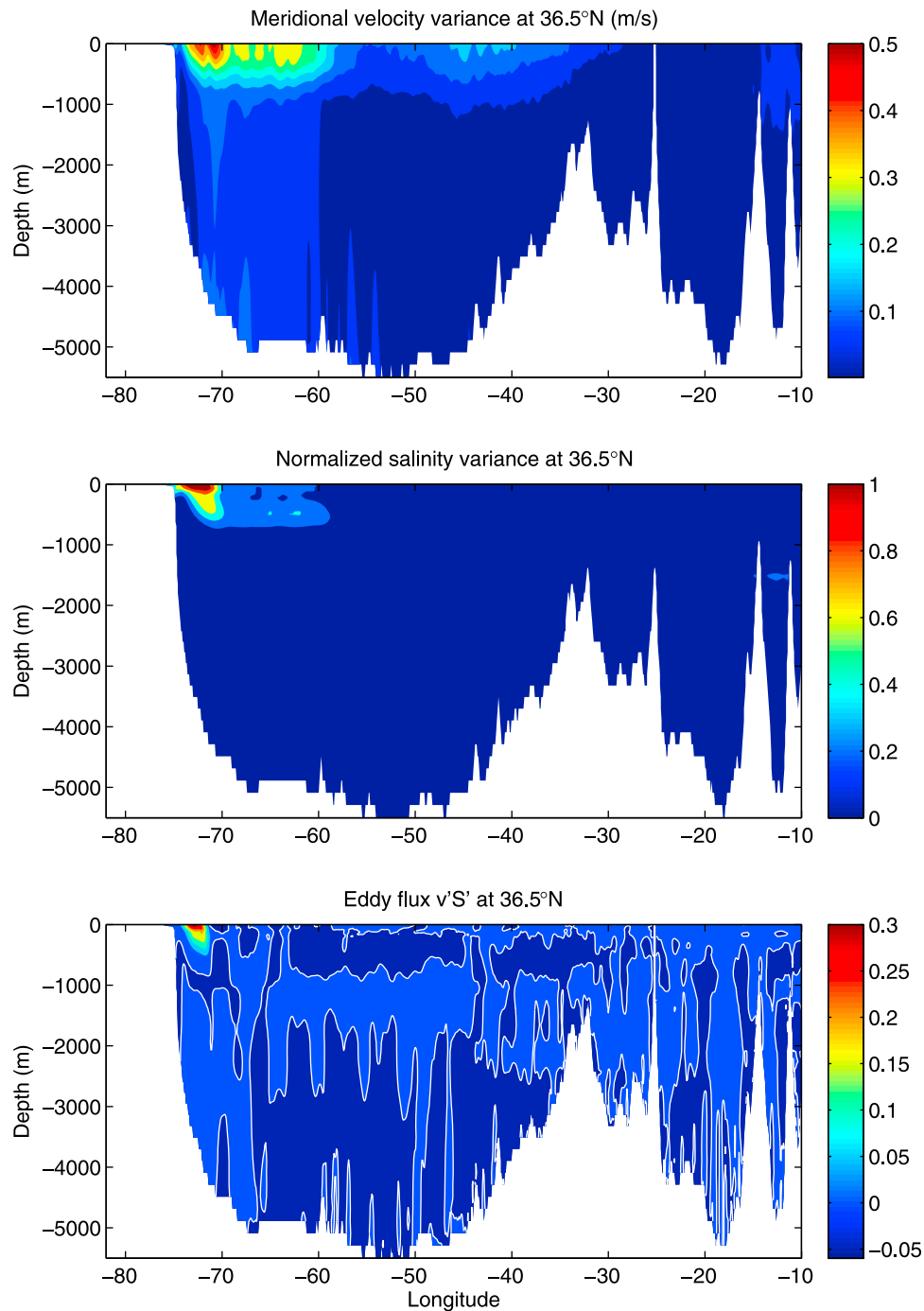


Figure 10. Variance of velocity in NATL12, normalized salinity S/S_0 and eddy flux averaged over the 1993–2004 period, along the section at 36.5°N (the zero contour is indicated in white).

maximum northward eddy salt transport, and 15°N to the minimum. Figure 9 confirms the striking difference between latitude band 15°N – 26.5°N , where eddy salt flux divergence is important at all longitudes, and latitude band 33°N – 36.5°N , where most of the eddy salt flux divergence occurs next to the western boundary.

[35] Having established that the large local eddy salt flux near 36.5°N in NATL12 is mainly divergent, we compare its structure in Figure 10 with the variance of velocity and the variance of salinity (divided by S_0). The maximum velocity

and salinity variances are concentrated in the western boundary current, where the Gulf Stream separates from the coast near Cape Hatteras, and so is the eddy salt flux. This is confirmed by a map of depth-integrated eddy salt flux (Figure 11). From the map and the section, it appears clearly that the basin-wide meridional eddy salt flux results from the large positive flux on the western flank of the Gulf Stream in the upper layers. After its separation from the coast at Cape Hatteras, the Gulf Stream axis shifts with time and meanders develop downstream. The variability of the axis position

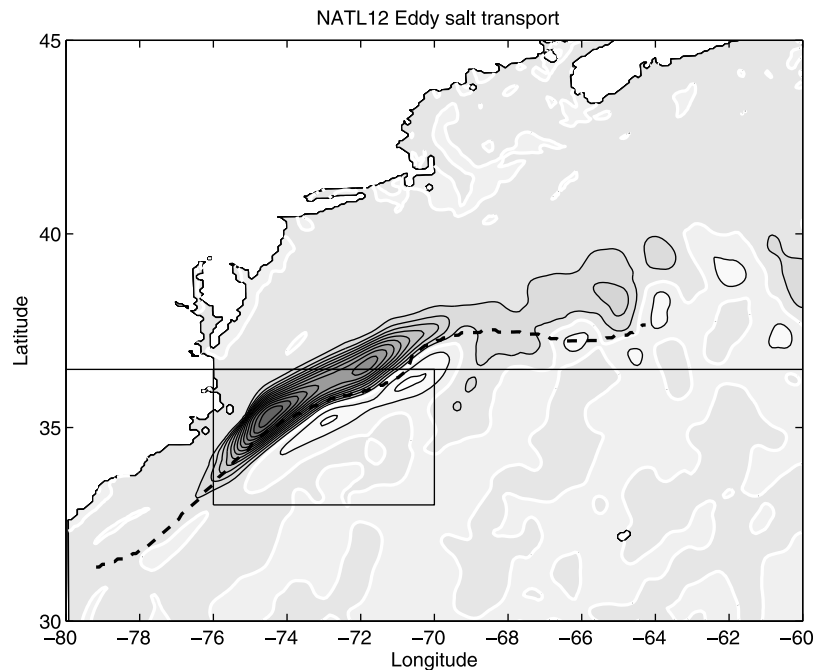


Figure 11. Map of normalized meridional eddy salt transport $v'S'/S_0$ in NATL12, integrated over depth and averaged over the 1993–2004 period in the Gulf Stream separation region. Contour interval is 0.002 Sv, the zero contour is outlined in white, positive values are indicated by a darker grey. The mean position of the Gulf Stream axis (maximum velocity at 200 m) is indicated by the thick black dashed line. The 36.5°N section is indicated, as well as the box where the flux divergence is integrated (see text).

leads to a characteristic “double blade” pattern of maximum eddy velocities around 72°W, 37°N with two maxima, one on each side of the mean jet axis, which are well observed by satellite altimetry [Ducet and Le Traon, 2001]. The NATL12 model reproduces this pattern (not shown). However, contrary to the symmetry of the eddy velocities, the positive eddy salt flux on the west side of the jet is much larger than the negative flux on the other side (Figure 11) which leads to the large positive basin-averaged meridional eddy flux at 36.5°N. Let us stress again that this local eddy flux is divergent: indeed the divergence of the eddy salt flux integrated in the box shown in Figure 11, 0.32 Sv, represents 90% of the eddy salt flux divergence integrated in that latitude band over the whole basin, and Figure 9 confirms that there are no other significant contributions to the divergence east of this box. The eddy heat transport behaves similarly to the eddy salt transport (not shown).

[36] Compared with other models, the strength of the eddy effect at these latitudes is especially large in NATL12 (we already noted in section 2.2 that the eddy heat transport in NATL12 is larger than in the POP model of Hecht and Smith [2008]). This eddy effect for both heat and salt is subject to a large interannual variability (as shown in Figure 6a), and furthermore, it is dependent on the model simulation (in a companion NATL12 experiment, not shown, the eddy heat transport at 36.5°N can be lower by about 50% depending on the period considered). For these reasons, it is necessary to investigate the robustness of this effect in new numerical experiments and to perform a more detailed validation of the modeled Gulf Stream separation: these studies are now under way. Here we just confirm by Figures 10 and 11 the

importance of the western boundary current separation for transient eddy transports, a feature that was pointed out earlier by Drijfhout [1994] in an idealized basin model.

[37] Let us now consider the 15°N section (Figure 12). The velocity variance is larger in the Caribbean Sea (west of 60°W), and above 1000 m. The salinity variance is large everywhere along the section in the upper layers (in the top 500 m). The eddy salt flux is negative over a large fraction of the section, excepted for large positive values near the surface in the Caribbean Sea; these are compensated by negative values below so that the net contribution of the Caribbean Sea to the zonal integral is small (Figure 7). In agreement with Figure 8, 88% of the total integrated $\overline{v'S'}$ flux is found in the top 500 m, where velocity and salinity fluctuations are anticorrelated (correlation coefficients of -0.2 to -0.4). The fluctuations are characterized by westward propagating anomalies (not shown), with typical zonal wavelengths of 200 km and timescales of one or two months. This is consistent with the baroclinic instabilities developing on the westward return branch of the subtropical gyre as found by Cox [1985] in his idealized model of a rectangular basin. Indeed, in our model salt fluxes and temperature fluxes have similar longitudinal structure, when averaged over the depth. Like the salt fluxes, the temperature fluxes are spread zonally over the section, concentrated in the upper 500 m (72% of the total), and the velocity-temperature anticorrelation has a magnitude similar to the velocity-salinity anticorrelation. Baroclinic instability is thus likely responsible for both the eddy heat and the eddy salt transport at this latitude. It certainly plays an important part at the northern boundary of the gyre (42°N) as well, as

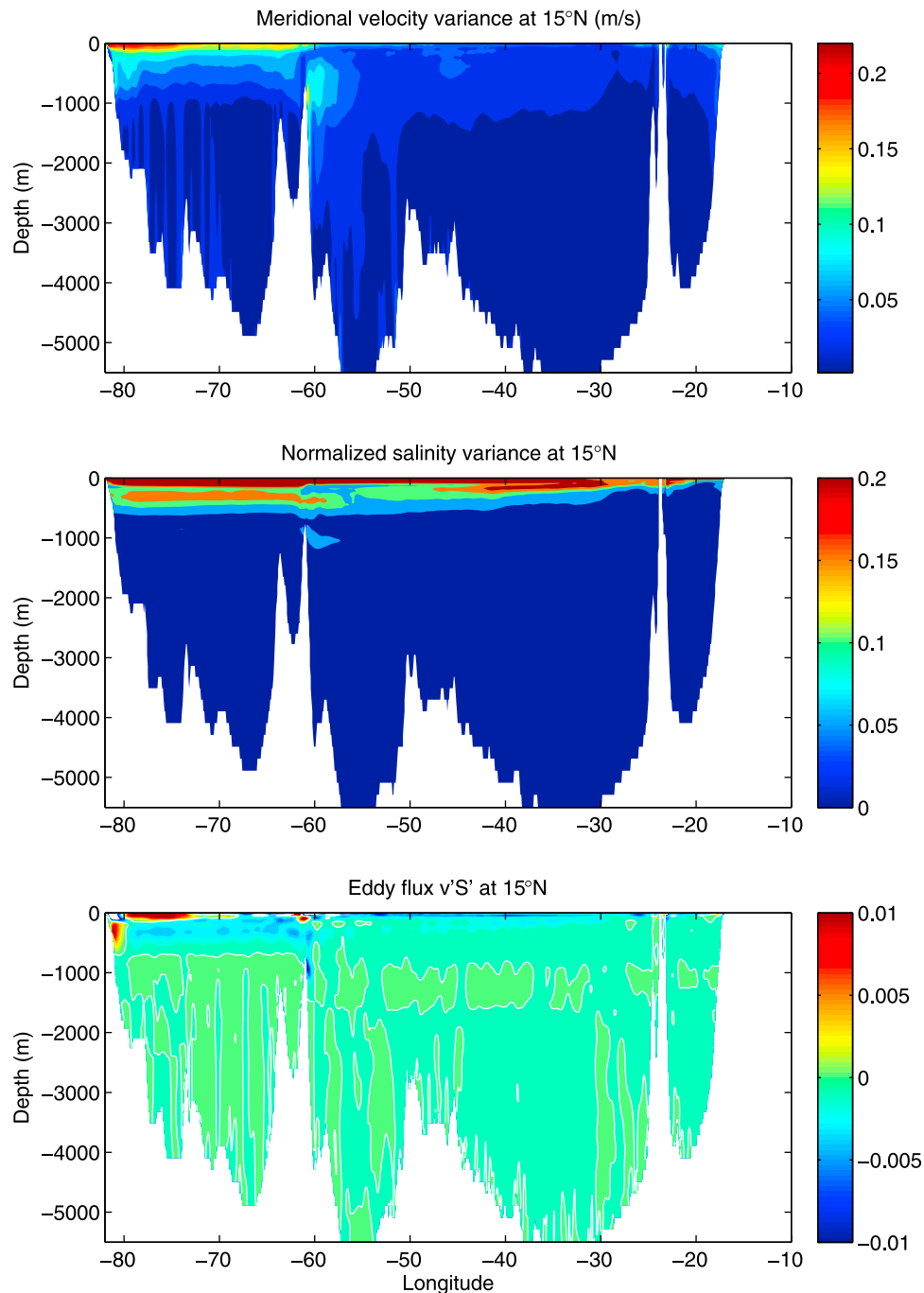


Figure 12. Variance of velocity in NATL12, normalized salinity S/S_0 and eddy flux averaged over the 1993–2004 period, along the section at 15°N (the zero contour is indicated in white).

shown by the repartition of eddy salt fluxes all along the section as is the case at 15°N (Figure 7).

[38] Following the theory of *Gent et al.* [1995], the fluxes generated by baroclinic instability are both advective (advection by the eddy-induced velocity) and diffusive (diffusion of temperature and salinity anomalies along isopycnals). In order to understand better the implications for parameterizing these fluxes in climate models, it is useful to separate these effects as done by *Lee et al.* [2007] in a model of the Southern Ocean. The method starts from the

conservation equations for a tracer (here salinity, S) in an isopycnal framework [see also *Gent et al.*, 1995]

$$\frac{\partial}{\partial t}(Sh) + \nabla(\mathbf{u}hS) = \mathcal{H}, \quad (9)$$

with h the isopycnal layer thickness and \mathcal{H} designating the source and sink terms as well as sub-grid scale diffusion. We note the time-average by an overbar, and the thickness-weighted average of a variable v by a caret, such as $\hat{v} = \overline{vh}/\bar{h}$.

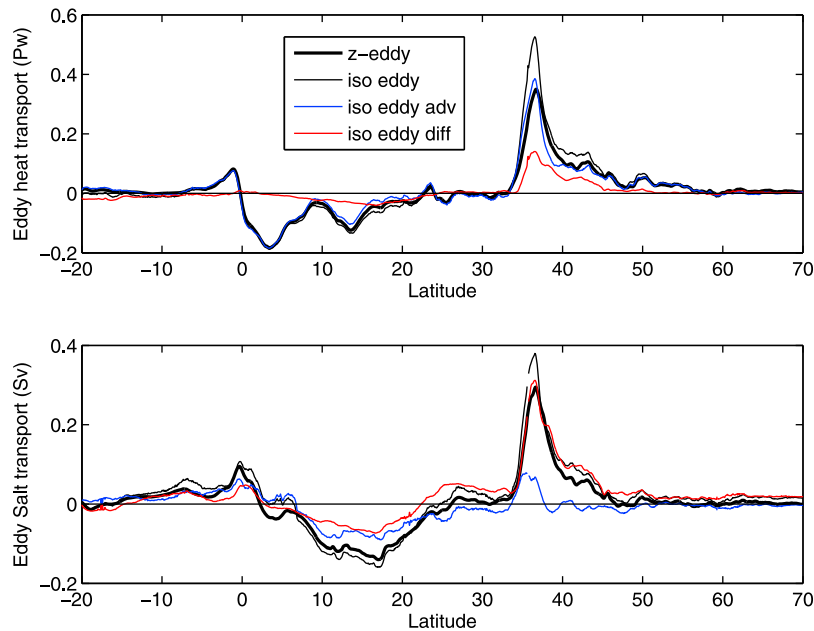


Figure 13. Total eddy flux in NATL12 calculated in z -coordinates (thick black curve, same as Figure 6) as well as in isopycnal coordinates (thin black curve, see text for definition). The separate contributions of eddy advection (blue) and diffusion (red) in isopycnal coordinates are also indicated, for (top) heat and (bottom) normalized salt transport.

The double prime is a deviation from the thickness-weighted average: $v'' = v - \hat{v}$. Using these notations, the time-averaged advective flux of tracer can be decomposed into an advective and a diffusive part

$$\overline{\mathbf{u}h\bar{S}} = \hat{\mathbf{u}}\hat{S}\bar{h} + \overline{\mathbf{u}''S''\bar{h}}. \quad (10)$$

A velocity component \hat{v} can be further decomposed into a Eulerian mean and an eddy-induced velocity [Gent *et al.*, 1995]

$$\hat{v} = \bar{v} + \frac{\overline{v'h'}}{\bar{h}} = \bar{v} + v_e, \quad (11)$$

where v_e is the eddy-induced velocity. Thus, the first term of the rhs in (10) contains an eddy advective tracer flux due to velocity-thickness correlations (advection of S by \mathbf{u}_e) and the second term is diffusion of tracer along isopycnals resulting from the triple correlation of velocity, thickness and tracer. These terms can be estimated in a z -coordinate model (as done by Lee *et al.* [2007]) by binning the instantaneous model output into isopycnal layers and calculating the time-averages. We have performed the same analysis for our best-resolved model, NATL12, using 93 bins of potential density σ_1 referenced to 1000 m. The method ensures that a sum of the total tracer transport $\overline{\mathbf{u}h\bar{S}}$ over the isopycnal bins gives exactly the same transport as a vertical integral over the model z -levels. The advective, diffusive and total fluxes of heat and salt are represented as a function of latitude in Figure 13. The eddy transports calculated in z -coordinates shown previously in Figures 3 and 6 are superimposed for comparison. There is a difference between the z -coordinate eddy flux and the isopycnal definition of the eddy flux. As pointed out by Lee *et al.* [2007] it is due to the difference between the eulerian mean

tracer \bar{S} used to define $\overline{v'S'}$ and the thickness-weighted averaged tracer \hat{S} used to define $v''S''$. The difference is rather small because these two averages are not fundamentally different for temperature and salinity.

[39] This advective-diffusive decomposition has never been performed in the North Atlantic, therefore we document not only the salt transport but also the the heat transport (Figure 13, top). For heat, the diffusive part is much smaller than the advective part, excepted in the 35–40°N latitude band. Indeed the advective component (blue curve on Figure 13, top) is undistinguishable from the total (thin black curve) in some latitude bands. In the subtropical gyre, temperature is an active tracer, whose fluctuations are linked with fluctuations of the density field, so that the eddy transport is almost completely explained by the velocity-thickness correlations. Note that this is not in contradiction with Stammer’s [1998] analysis based on a diffusive hypothesis and large scale horizontal gradients of temperature, because at first order, within the quasi-geostrophic approximation, advection by eddy-induced velocities is not distinguishable from horizontal diffusion [Treguier *et al.*, 1997]. In the “quasi-geostrophic diffusion” view, eddies mix the temperature downgradient, exporting heat out of the subtropical gyre. In the “eddy-advection” view, eddy-induced velocities tend to flatten the bowl-shaped isopycnals of the subtropical gyre, flushing light (and warm) water out of it. Both views are consistent with the sign of the eddy heat flux. Our model confirms the key role of velocity-thickness correlations and supports the use of the parameterization of Gent *et al.* [1995] in low resolution primitive-equation models of the North Atlantic.

[40] Regarding the salt transport (Figure 13, bottom), the diffusive component is more important. This is consistent with the fact that density is primarily determined by temperature in

the subtropical gyre, and that large salinity gradients and salinity fluctuations can develop along isopycnals. The isopycnal diffusion of salt is much larger than the advective component in the Gulf Stream and north Atlantic system (35 to 45°N). This is consistent with the existence of large salinity gradients along isopycnals in the upper ocean at these latitudes. As pointed out by *Lee et al.* [2007] the advective and diffusive eddy contributions to salt transport are not always of the same sign; they can reinforce or oppose each other, depending on the horizontal and vertical gradients of salinity. Opposing effects occur at 26°N where the eddy advective salt flux is to the south and the eddy diffusive flux to the north, leading to a small total eddy salt flux. This behavior demonstrates that the effect of eddies is more complex than a simple downgradient mixing.

[41] We do not estimate eddy mixing coefficients here as *Lee et al.* [2007] did, because a zonally averaged view is less relevant in the North Atlantic than in the Antarctic Circumpolar current, and performing a three-dimensional calculation would require eliminating the rotational components of the fluxes. This has been attempted by C. Eden in a high resolution model of the North Atlantic, with success in the case of the thickness fluxes [*Eden et al.*, 2007] but not in the case of the isopycnal diffusion of tracers [*Eden and Greatbatch*, 2009]. *Eden and Greatbatch* [2009] found that the eddy mixing coefficients are highly non-isotropic, the meridional mixing coefficient being smaller than the zonal one.

5. Discussion and Conclusion

[42] The purpose of our study was to document, for the first time, the eddy contribution to the meridional transport of salt in the North Atlantic in an eddy resolving model at 1/12° resolution (NATL12). A preliminary step was to diagnose the total transports of heat, salt and volume, and validate them using observations. The comparison of NATL12 with lower resolution models showed that both volume transport and salt transport depend on model resolution, just like heat transport whose dependency on model resolution has been known for more than 10 years.

[43] The eddy velocity-salinity correlations contribute to a significant salt transport in the subtropical gyre. Between 15°N and the center of the gyre where the eddy transport of salt vanishes, the divergence of eddy salt transport of -0.15 Sv in the NATL12 model is very significant compared with the net evaporation of 0.31 Sv over this latitude band. Considering the whole subtropical region from 10°N to 40°N, the eddy salt flux divergence of 0.2 Sv is of the same order of magnitude as the net upward water flux (0.6 Sv). We emphasize that eddy salt transports cannot be ignored at midlatitudes in eddy models. However, the model eddy salt fluxes, like eddy heat fluxes, are small in the subpolar gyre. This may be due to the smaller meridional gradients (rather, the subpolar gyre is characterized by strong zonal gradients of temperature and salt) or to the fact that our spatial resolution of 1/12° is still too coarse to resolve eddies in the subpolar oceans, where the Rossby deformation radius is small.

[44] Near 15°N, the southward eddy salt flux reaches -5.2 Sv.PSU, or -0.15 Sv when normalized by a reference salinity. This eddy salt flux is consistent with the calculation by *Stammer* [1998] based on an eddy mixing coefficient and

a diffusive hypothesis. *Stammer's* maximum southward eddy transport in the Atlantic (his Figure 8b) was located closer to the equator (near 10°N) and smaller than ours (-1.10^8 kg/s, corresponding to -0.1 Sv) but the agreement for the order of magnitude between the two independent estimates is encouraging. However, a separate calculation of the advective and diffusive contributions to the total eddy transport in an isopycnal framework confirms that the effect of eddies should not be viewed as a simple horizontal diffusion. Rather, it is consistent with the advective-diffusive parameterization of *Gent et al.* [1995] used by most climate models. At the northern boundary of the subtropical gyre, around 36–42°N, the eddy flux has a magnitude similar to the flux at 15°N but an opposite sign (to the north). When eddy fluxes are spread over a large area of the meridional section, as happens at 15°N and 42°N, they are consistent with the mechanism that has been invoked in all previous studies of eddy heat flux, namely, baroclinic instability of the mean flow.

[45] The meridional structure of salt transports shows a large compensation between the eddy and mean components. Both have anti-correlated variations as a function of latitude. In ice-free regions, this compensation happens necessarily if the eddy fluxes are an order of magnitude larger than the temporal changes in salt content and the parameterized lateral diffusion of salt. The compensation was much less clear in some previously published model results, such as *McCann et al.* [1994] or *Meijers et al.* [2007] because these models had been integrated for a short period of time so that the drift was probably very strong. Here we have demonstrated a quasi-perfect compensation between the eddy and the mean transports of salt in the subtropical gyre in a global model experiment at lower resolution (1/4°) that has been run for 327 years with a climatological forcing, thus allowing the model to equilibrate better and the drift to become much smaller.

[46] The consistency of our results with *Stammer* [1998] suggests that the divergence of the eddy salt transport in the real ocean may indeed represent a few tens of Sv in the subtropical Atlantic. However, if this is the case, this large eddy transport must be compensated by the transport of salt by the mean currents, in order to be compatible with the observed variability of salt content (which is typically smaller than the drift found in the NATL12 model). If the amplitude of our model eddy salt transport is realistic, and the good compensation between eddy and mean is realistic as well, this raises two questions. First, are the salt transports measurable in the ocean? Besides the main source of uncertainty for salt transports which is the difficulty to measure the net mass transports, the presence of an eddy contribution compensating the transport by the mean flow is another difficulty which has been ignored until now, but will have to be taken into account when in-situ measurements are used to provide information on salt transports. The second question is the mechanisms by which the compensation operates and the timescales involved, because this could have important consequences for the evolution of climate. Regarding the baroclinic instability mechanisms at play for example at 15°N, we have not explored their variability over long (decadal) timescales due to the relatively short duration of the high resolution NATL12 experiment (25 years).

[47] A specific feature of the NATL12 model is the presence of a large peak of eddy transport at 36.5°N, near the latitude at which the Gulf Stream separates from the coast at Cape Hatteras. This large eddy contribution is found for the heat transport as well as the salt transport. It is model-dependent, and much weaker at lower resolution in the 1/4° models. We have shown that this eddy contribution occurs in a very limited region on the western flank of the Gulf Stream. NATL12 may be an extreme example of this eddy effect, but it is likely occurring in other models as well: indeed an early study of *Drijfhout* [1994] pointed out the importance of the western boundary current for the meridional heat flux in an idealized model. If the same variability happens in the ocean it has implications for observation of eddy fluxes. *Wunsch* [1999] used current meter data to assess the importance of eddies for the meridional heat transport and found significant fluxes in the western boundary currents. However, the significance of these eddy fluxes cannot be understood unless the extent of eddy/mean compensation in western boundary currents is quantified; large eddy transports can occur locally with no consequence for the basin wide meridional transport if they are compensated by opposing mean transports.

[48] In coupled climate models the transport of heat and salt by eddies has been usually parameterized, because the ocean components of earth system models did not have enough resolution to represent eddies. One could be tempted to conclude from our analysis that the present parameterizations of eddy transports in climate models are adequate to represent the effects of eddies, but it is not the case. The comparison of models at different resolution (1/4° to 1/12°) shows that the total heat and volume transports vary with resolution, and only NATL12 has a heat transport at 26°N compatible with the recent observations of the RAPID array [*Johns et al.*, 2011]. The changes occur mainly through modifications of the mean currents as the spatial resolution of the model is increased, leading to changes in the air-sea fluxes (changes in heat loss by evaporation, for example). The modifications of the circulation at higher resolution are due to a better representation of the bathymetry, a decreased viscosity, but also to indirect effects of the eddies themselves, for example the tendency for eddy momentum fluxes to amplify eastward jets in the ocean [*Levy et al.*, 2010]. The current effort to increase the resolution of ocean models for climate simulations and climate change scenarios is thus necessary.

[49] **Acknowledgments.** This work is a contribution of the Drakkar project, which is funded by the Centre National de la Recherche Scientifique (CNRS), the Institut National des Sciences de l'Univers (INSU), the Groupe Mission Mercator Coriolis (GMMC) and Ifremer. Computations presented in this study were performed at computing centers operated by GENCI: Institut du Développement et des Ressources en Informatique Scientifique (IDRIS) and Centre Informatique National de l'Enseignement Supérieur (CINES). We thank Sébastien Theetten and Catherine Guivarc'h for their help in the development of the NATL12 model. We thank Lynne Talley for useful discussions about the freshwater transports and three anonymous reviewers whose comments have helped improved the manuscript.

References

- Barnier, B., et al. (2006), Impact of partial steps and momentum advection schemes in a global ocean circulation model at eddy-permitting resolution, *Ocean Dyn.*, 56(5–6), 543–567.
- Brodeau, L., B. Barnier, A. Treguier, T. Penduff, and S. Gulev (2010), An ERA40-based atmospheric forcing for global ocean circulation models, *Ocean Modell.*, 31, 88–104, doi:10.1016/j.ocemod.2009.10.005.
- Bryan, F. O., and R. D. Smith (1998), Modeling the north atlantic circulation: From eddy-permitting to eddy-resolving, *Int. WOCE Newsl.*, 33, 12–14.
- Bryan, K. (1986), Poleward buoyancy transport in the ocean and mesoscale eddies, *J. Phys. Oceanogr.*, 16, 927–933.
- Cox, M. (1985), An eddy resolving model of the ventilated thermocline, *J. Phys. Oceanogr.*, 15, 1312–1324.
- Curry, R., B. Dickson, and I. Yashayaev (2003), A change in the freshwater balance of the Atlantic Ocean over the past four decades, *Nature*, 426, 826–829.
- Dai, A., and K. Trenberth (2002), Estimates of freshwater discharge from continents: Latitudinal and seasonal variations, *J. Hydrometeorol.*, 3, 660–687.
- Dickson, R., B. Rudels, S. Dye, M. Karcher, J. Meinck, and I. Yashayaev (2007), Current estimates of freshwater flux through Arctic and subarctic seas, *Prog. Oceanogr.*, 73, 210–230.
- Drakkar Group (2007), Eddy permitting ocean circulation hindcasts of past decades, *Clivar Exch.*, 42, 8–10.
- Drijfhout, S. (1994), Heat transport by mesoscale eddies in an ocean circulation model, *J. Phys. Oceanogr.*, 24, 353–369.
- Ducet, N., and P. Le Traon (2001), A comparison of surface eddy kinetic energy and Reynolds stresses in the Gulf Stream and the Kuroshio current systems from merged TOPEX/Poseidon and ERS-1/2 altimetric data, *J. Geophys. Res.*, 106, 16,603–16,622.
- Ducet, N., P. Y. Le Traon, and G. Reverdin (2000), Global high-resolution mapping of ocean circulation from TOPEX/Poseidon and ERS-1 and -2, *J. Geophys. Res.*, 105, 19,477–19,498.
- Eden, C., and H. Dietze (2009), Effects of mesoscale eddy/wind interactions on biological new production and eddy kinetic energy, *J. Geophys. Res.*, 114, C05023, doi:10.1029/2008JC005129.
- Eden, C., and R. Greatbatch (2009), A diagnosis of isopycnal mixing by mesoscale eddies, *Ocean Modell.*, 27, 98–106.
- Eden, C., R. Greatbatch, and J. Willebrand (2007), A diagnosis of thickness fluxes in an eddy-resolving model, *J. Phys. Oceanogr.*, 37, 727–742.
- Fox-Kemper, B., R. Ferrari, and J. Pedlosky (2003), On the indeterminacy of rotational and divergent eddy fluxes, *J. Phys. Oceanogr.*, 33, 478–483.
- Ganachaud, A., and W. Wunsch (2003), Large scale ocean heat and freshwater transports during the World Ocean Circulation Experiment, *J. Clim.*, 16, 696–705.
- Gent, P., J. Willebrand, T. McDougall, and J. McWilliams (1995), Parameterizing eddy-induced tracer transports in ocean circulation models, *J. Phys. Oceanogr.*, 25, 463–474.
- Grist, J. P., et al. (2010), The roles of surface heat flux and ocean heat transport convergence in determining Atlantic Ocean temperature variability, *Ocean Dyn.*, 60, 771–790.
- Hawkins, E., R. Smith, L. C. Allison, J. M. Gregory, T. J. Woollings, H. Pohlmann, and B. de Cuevas (2011), Bistability of the Atlantic overturning circulation in a global climate model and links to ocean freshwater transport, *Geophys. Res. Lett.*, 38, L10605, doi:10.1029/2011GL047208.
- Hecht, M., and R. Smith (2008), Towards a physical understanding of the North Atlantic: A review of model studies, in *Ocean Modeling in an Eddying Regime*, *Geophys. Monogr. Ser.*, vol. 177, edited by M. W. Hecht and H. Hasumi, pp. 213–240, AGU, Washington, D. C.
- Huang, R., and R. W. Schmitt (1993), The Goldsbrough-Stommel circulation of the world oceans, *J. Phys. Oceanogr.*, 23, 1277–1284.
- Huisman, S. E., M. den Toom, H. A. Dijkstra, and S. Drijfhout (2010), An indicator of the multiple equilibria regime of the Atlantic meridional overturning circulation, *J. Phys. Oceanogr.*, 40, 551–567, doi:10.1175/2009JPO4215.1.
- Johns, W. E., et al. (2011), Continuous, array-based estimates of Atlantic Ocean heat transport at 26.5°N, *J. Clim.*, 24, 2429–2449.
- Kuo, H. (1956), Forced and free meridional circulations in the atmosphere, *J. Meteorol.*, 13, 561–568.
- Large, W. G., and S. G. Yeager (2009), The global climatology of an inter-annually varying air-sea flux data set, *Clim. Dyn.*, 33, 341–364, doi:10.1007/s00382-008-0441-3.
- Lee, M., A. Nurser, A. Coward, and B. de Cuevas (2007), Eddy advective and diffusive transports of heat and salt in the Southern Ocean, *J. Phys. Oceanogr.*, 37, 1376–1393.
- Levitus, S., T. P. Boyer, M. E. Conkright, T. O'Brien, J. Antonov, C. Stephens, L. Stathopoulos, D. Johnson, and R. Gelfeld (1998), *World Ocean Database 1998*, vol. 1, *Introduction*, NOAA Atlas NESDIS, vol. 18, 346 pp., NOAA, Silver Spring, Md.
- Levy, M., P. Klein, A. Treguier, D. Iovino, G. Madec, S. Masson, and K. Takahashi (2010), Modification of gyre circulation by sub-mesoscale physics, *Ocean Modell.*, 34, 1–15, doi:10.1016/j.ocemod.2010.04.001.
- Lique, C., A. Treguier, M. Scheinert, and T. Penduff (2009), A model-based study of ice and freshwater transport variabilities along both sides of Greenland, *Clim. Dyn.*, 33, 685–705, doi:10.1007/s00382-008-0510-7.

- Madec, G. (2008), NEMO ocean engine, *Note Pole Model. 27*, Inst. Pierre-Simon Laplace, Paris.
- McCann, M. P., A. Semtner, and R. Chervin (1994), Transports and budgets of volume, heat and salt from a global eddy-resolving ocean model, *Clim. Dyn.*, *10*, 59–80.
- Meijers, A. J., N. L. Bindoff, and J. Robert (2007), On the total, mean and eddy heat and freshwater transports in the Southern Hemisphere of a $1/8^\circ \times 1/8^\circ$ global ocean models, *J. Phys. Oceanogr.*, *37*, 277–295.
- Penduff, T., M. Juza, B. Barnier, J. Zika, W. Dewar, A. Treguier, J. Molines, and N. Audiffren (2011), Sea-level expression of intrinsic and forced ocean variabilities at interannual time scales, *J. Clim.*, *24*, 5652–5670.
- Rattan, S., P. G. Myers, A.-M. Treguier, S. Theetten, A. Biastoch, and C. Boening (2010), Towards an understanding of Labrador Sea salinity drift in eddy-permitting simulations, *Ocean Modell.*, *35*(1–2), 77–88.
- Roullet, G., and G. Madec (2000), Salt conservation, free surface, and varying levels: A new formulation for ocean general circulation models, *J. Geophys. Res.*, *105*, 23,927–23,942.
- Smith, R. D., M. E. Maltrud, F. O. Bryan, and M. Hecht (2000), Simulation of the North Atlantic Ocean at $1/10^\circ$, *J. Phys. Oceanogr.*, *30*, 1532–1561.
- Stammer, D. (1998), On eddy characteristics, eddy transports, and mean flow properties, *J. Phys. Oceanogr.*, *28*, 727–739.
- Talley, L. D. (2008), Freshwater transport estimates and the global overturning circulation: Shallow, deep, and throughflow components, *Prog. Oceanogr.*, *78*, 257–303.
- Treguier, A. (2008), Drakkar natl12 model configuration for a 27-year simulation of the North Atlantic Ocean, *Drakkar Rep. LPO-2008-05*, Lab. de Phys. des Oceans, Cent. Natl. de la Rech. Sci., Brest, France. [Available at <http://www.drakkar-ocean.eu/publications/reports/>]
- Treguier, A., I. Held, and V. Larichev (1997), Parameterization of quasigeostrophic eddies in primitive equation ocean models, *J. Phys. Oceanogr.*, *27*(4), 567–580.
- Treguier, A. M., et al. (2001), An eddy permitting model of the Atlantic circulation: Evaluating open boundary conditions, *J. Geophys. Res.*, *106*, 22,115–22,129.
- Treguier, A. M., M. England, S. R. Rintoul, G. Madec, J. Le Sommer, and J.-M. Molines (2007), Southern Ocean overturning across streamlines in an eddy simulation of the Antarctic Circumpolar Current, *Ocean Sci.*, *3*, 491–507.
- Treguier, A., J. L. Sommer, J. Molines, and B. de Cuevas (2010), Response of the Southern Ocean to the southern annular mode: Interannual variability and multidecadal trend, *J. Phys. Oceanogr.*, *40*, 1659–1668.
- Treguier, A., B. Ferron, and R. Dussin (2012), Buoyancy driven currents in eddy ocean models, in *Buoyancy-Driven Flows*, edited by E. Chassignet, C. Cenedese, and J. Verron, pp. 281–311, Cambridge Univ. Press, Cambridge, U. K.
- Trenberth, K. E., and D. P. Stepaniak (2003), Covariability of components of poleward atmospheric energy transports on seasonal and interannual timescales, *J. Clim.*, *16*, 3691–3705.
- Tsimplis, M. N., M. Marcos, and S. Somot (2008), 21st century Mediterranean Sea level rise: Steric and atmospheric pressure contributions from a regional model, *Global Planet. Change*, *63*, 105–111.
- van Loon, H. (1979), The association between latitudinal temperature gradient and eddy transport. Part I: Transport of sensible heat in winter, *Mon. Weather Rev.*, *107*, 525–534.
- Wijffels, S. (2001), Ocean transport of fresh water, in *Ocean Circulation and Climate, Int. Geophys. Ser.*, vol. 77, edited by G. Siedler, J. Church, and J. Gould, pp. 475–488, Academic, London.
- Woodgate, R. A., and K. Aagaard (2005), Revising the Bering Strait freshwater flux into the Arctic Ocean, *Geophys. Res. Lett.*, *32*, L02602, doi:10.1029/2004GL021747.
- Wunsch, C. (1999), Where do ocean eddy heat fluxes matter, *J. Geophys. Res.*, *104*, 13,235–13,249.